Cell Transplantation, Vol. 22, pp. 1337–1349, 2013

0963-6897/13 $90.00 + .00
DOI: http://dx.doi.org/10.3727/096368912X657657
E-ISSN 1555-3892
www.cognizantcommunication.com

Human Amnion Epithelial Cells Repair Established Lung Injury

Patricia Vosdoganes,*† Euan M. Wallace,*† Siow Teng Chan,*
Rutu Acharya,* Tim J. M. Moss,*† and Rebecca Lim*

*The Ritchie Centre, Monash Institute of Medical Research, Monash University, Clayton, Victoria, Australia
†Department of Obstetrics and Gynecology, Monash Medical Centre, Monash University, Clayton, Victoria, Australia

With a view to developing a cell therapy for chronic lung disease, human amnion epithelial cells (hAECs) have been shown to prevent acute lung injury. Whether they can repair established lung disease is unknown. We aimed to assess whether hAECs can repair existing lung damage induced in mice by bleomycin and whether the timing of cell administration influences reparative efficacy. In addition, we aimed to characterize the effect of hAECs on fibroblast proliferation and activation, investigating possible mechanisms of reparative action. hAECs were administered intraperitoneally (IP) either 7 or 14 days after bleomycin exposure. Lungs were assessed 7 days after hAEC administration. Bleomycin significantly reduced body weight and induced pulmonary inflammation and fibrosis at 14 and 21 days. Delivery of hAECs 7 days after bleomycin had no effect on lung injury, whereas delivery of hAECs 14 days after bleomycin normalized lung tissue density, collagen content, and α-SMA production, in association with a reduction in pulmonary leucocytes and lung expression of TGF-β, PDGF-α, and PDGF-β. In vitro, hAECs reduced proliferation and activation of primary mouse lung fibroblasts. Our findings suggest that the timing of hAEC administration in the course of lung disease may impact on the ability of hAECs to repair lung injury.

Key words: Amnion epithelial cells; Bleomycin; Fibrosis; Inflammation; Chronic lung disease; Regenerative medicine

INTRODUCTION

A recent World Health Organization (WHO) report estimated that over 300 million people suffer chronic lung diseases worldwide (45). While public health initiatives rightly focus on prevention, few treatment options exist for those individuals with established lung disease. Current therapies, such as corticosteroids, are essentially limited to providing symptomatic relief, rather than lung repair (3,6,30). As such, there is a pressing need for novel reparative treatments for those with established lung injury and thereby improve quality of life. Over the last decade, there have been an increasing number of studies evaluating cell-based therapies as a possible treatment for chronic lung disease, including studies using cells obtained from gestational tissues, such as the placenta (4,11,33,35).

Human amnion epithelial cells (hAECs), sourced from the term amniotic membrane, are a particularly attractive candidate for cell therapy. Morphologically, hAECs maintain a normal karyotype in culture (29) and, unlike embryonic stem cells (ESCs), they do not form teratomas in vivo (17,29). They are also considered "immune privileged," lacking expression of major histocompatibility complex (MHC) class II or highly polymorphic human leukocyte antigens (HLAs) (16,17), a property likely stemming from their early developmental origins. This will allow allogeneic use without the need for immunosuppression, as confirmed by the success in allogeneic transplantation in human disease (1) and xenotransplantation in animal models (35,44) without evidence of immune rejection. Furthermore, hAECs are abundant and pose no ethical concerns regarding their collection (11,36). The term placenta is essentially medical waste and in excess of 100 million cells can be extracted from each amnion.

There are two key properties of hAECs, suggesting their likely efficacy in the treatment of established lung injury—their pluripotency and their anti-inflammatory effects. hAECs harbor a pluripotency similar to ESCs with the capacity to generate multiple cell types (7,17,38) including pulmonary alveolar epithelial cells (AECs) (33,35). Engraftment and differentiation of transplanted hAECs into pulmonary epithelium has been demonstrated in mice exposed to bleomycin (4,33). However, low engraftment rates observed in recent studies of both adult (35) and fetal (44) lung disease suggests that hAECs are likely to primarily act via immune modulation rather than by in vivo differentiation. The anti-inflammatory characteristics

Received October 22, 2011; final acceptance August 10, 2012. Online prepub date: October 4, 2012.
Address correspondence to Dr. Rebecca Lim, The Ritchie Centre, Monash Institute of Medical Research, Level 3, 27-31 Wright Street, Clayton, Victoria 3168, Australia. Tel: +61 3 9594 7410; E-mail: Rebecca.Lim@monash.edu

of human amnion have been utilized for over 50 years to support wound healing in burns (2), surgical wounds (14), and corneal repair (8). In vitro, hAECs inhibit the activity of immune cells, including neutrophils, macrophages, and lymphocytes (23,34,46). Within the lung, such immune modulation has enabled hAECs to prevent acute lung injury in a variety of animal models (33,35,44). However, it remains unclear whether hAECs can repair established lung damage. There is a single report that hAECs reduced lung collagen deposition in severe combined immune deficient mice (SCID) mice following bleomycin lung injury (33) but whether such repair occurs in immune competent animals has not been explored.

Accordingly, we undertook the current study to assess whether hAECs can repair established bleomycin-induced lung fibrosis in immune competent mice and to explore whether the timing of cell administration relative to the injury onset altered the efficacy of the hAECs.

MATERIALS AND METHODS

In Vivo Studies

Animals and Experimental Groups. All experimental procedures were approved by the relevant Monash University Animal Ethics Committee and were conducted in accordance with the Australian Code of Practice for the Care and Use of Animals for Scientific Purposes (37).

We used an adult bleomycin-induced lung injury model, as previously described (35). Briefly, female C57Bl/6 mice aged 6–8 weeks, sourced from Monash Animal Services (Monash University, Victoria, Australia), were randomly assigned to one of four groups: *Saline alone* (*control*)—mice received intranasal (IN) saline with intraperitoneal (IP) injection of saline; *Bleomycin alone*—mice received IN bleomycin and IP injection of saline; *Saline + hAECs*—mice received IN saline and IP injection of hAECs; *Bleomycin + hAECs*—mice received IN bleomycin and IP injection of hAECs. Each group consisted of eight animals per treatment group per time point. Animals were further allocated at random to receive hAECs at either 7 or 14 days after bleomycin, as detailed below.

Mice were anesthetized by IP injection of xylazine (2 mg/kg) and ketamine (100 mg/kg; both from Provet WA Pty Ltd., Malaga, Australia). Bleomycin (Blenoxane, Bristol-Myers Squibb, New York, NY, USA) was administered 0.03 units/kg IN, reconstituted in sterile saline. Control animals received an equivalent volume of saline.

Human Amnion Epithelial Cell Preparation. Human amnion epithelial cells (hAECs) were isolated from term placentae donated by healthy women, aged 24–39 years, undergoing elective cesarean section, using procedures described previously (36). Briefly, the amnion was peeled manually from the chorion, rinsed of blood, and incubated in 0.05% trypsin (Gibco/Life Technologies, Mulgrave, Victoria, Australia) for cell digestion. Once isolated, hAEC viability was assessed by trypan blue (Gibco) exclusion: >80% viability was required. Epithelial cell purity was assessed by EpCam immunostaining (Becton Dickinson, North Ryde, NSW, Australia): purity >94% and cluster of differentiation 105 and 90 (CD105/CD90; primary antibodies from Becton Dickinson with secondary antibody anti-mouse 488 from Life Technologies; mesenchymal markers) <1% was required. Cells were resuspended to 4 million hAECs in 250 ml sterile saline. For the purpose of the in vivo studies, hAECs from three donor placentae were combined prior to administration to animals.

Injection Protocol and Study Timeline. To compare the effect of timing of hAEC administration on lung repair, 4 million hAECs were administered IP either 7 days (D7) or 14 days (D14) after intranasal bleomycin. Control animals received an equivalent volume of saline IP either D7 or D14. Animal well-being was monitored daily by observation and body weight. Animals were sacrificed 7 days after hAEC administration by carbon monoxide inhalation. That is animals receiving hAECs on D7 were culled on D14 and animals receiving hAECs on D14 were culled on D21. Figure 1 summarizes the experimental protocols.

Tissue Collection and Preparation. At tissue collection, the right lung was ligated at the right mainstem bronchus and the trachea exposed to allow instillation of 4% paraformaldehyde (PFA; Sigma-Aldrich, Sydney, Australia) into the left lung at 20 cm H_2O pressure. The left lung was excised and immersed in 4% PFA overnight before histological processing. The right lung was collected and snap-frozen in liquid nitrogen for subsequent molecular analysis. Lung tissue from each animal was analyzed for each experimental outcome and is represented within the

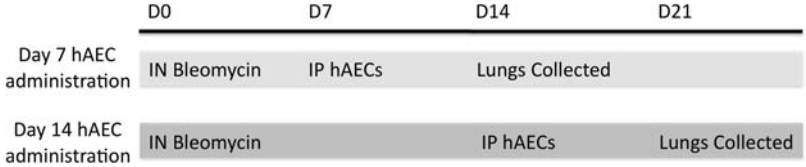

Figure 1. Graphical representation of treatment administration protocol. Bleomycin was administered intranasally (IN) at Day 0 (D0). Human amnion epithelial cells (hAECs) were administered by intraperitoneal (IP) injection on either D7 (experiment 1) or D14 (experiment 2). Animals were monitored for a further 7 days before lungs were collected on either D14 or D21, respectively.

data set. To account for the patchy lung lesions typical of bleomycin-induced injury, random subsampling for each experimental outcome was performed by finely chopping the lung tissues and allocating random pieces to each molecular analysis. Histological sections were cut to a thickness of 5 mm prior to staining.

Lung Morphology. One sagittal lung section from each mouse was stained with hematoxylin and eosin (H&E; Amber Scientific, Midvale, WA, Australia). Ten serial fields of view (200× magnification) were assessed by digital image analysis using the Image J software package (NIH, Bethesda, MA, USA) to determine the area tissue density, inclusive of cellular infiltrate, per field of view as previously described (26). Briefly, color digital images were obtained and converted to binary data, and the percentage of tissue pixels to whole lung pixels was calculated. The area occupied by tissue was then expressed as a percentage of total area of lung section.

Collagen Quantification. Histological sections were stained with Sirius Red (ProSciTech, Kirwan, QLD, Australia), as previously described (35). The area fraction of Sirius Red-positive tissue relative to total tissue area was quantified by digital image analysis using Image J software. Ten fields of view were assessed at 400× magnification.

CD45 Immunohistochemistry. Immunostaining on histological sections was performed using a rat anti-mouse CD45 monoclonal antibody (560501, 1:100, Becton Dickinson). Sections were blocked with a serum-free protein block (Dako, Campbellfield, Victoria, Australia) before primary incubation. Secondary staining was achieved using a goat anti-rat IgG antibody (AP1831b, 1:200, Chemicon, Billerica, MA, USA) and streptavidin–peroxidase conjugate with visualization by 3,3′-diaminobenzadine (both Dako). Area fraction of CD45-positive cells, as a proportion of total positive cell area per total cell area, was quantified using Image J software. Ten fields of view were assessed at 400× magnification.

Protein Isolation and Western Blotting. Total protein was extracted from frozen lung, and the protein concentration was determined using Pierce BCA protein assay (Thermo Fisher Scientific, Waltham, MA, USA). Western blot was performed using a rabbit anti-α-smooth muscle actin (α-SMA) polyclonal antibody (ab5694, 1:200, Abcam, Cambridge, UK). Protein (40 mg) was subjected to reducing sodium dodecyl sulfate polyacrylamide gel electrophoresis (SDS-PAGE; Life Technologies) and transferred onto a polyvinylidene difluoride (PVDF) membrane (Immobilon-P, Millipore, Billerica, MA, USA). Membranes were blocked with 5% skim milk powder (Fonterra, Otaga, New Zealand) in PBS/0.5% Tween-20 (PBS/T; Sigma-Aldrich) before primary incubation. Secondary staining was achieved using a goat anti-rabbit horse radish peroxidase (HRP) antibody (sc-2004, 1:10,000, Santa Cruz Biotechnology Inc., Santa Cruz, CA, USA). Bands were visualized using an Immobilon™ Western Chemiluminescent HRP substrate (Millipore) and quantified using the Quantity One™ quantitation analysis software (Bio-Rad Laboratories, Gladesville, NSW, Australia).

RNA Isolation and PCR Analysis. RNA was isolated from frozen lung tissue using TRIzol (Invitrogen, Carlsbad, CA, USA) and converted to cDNA using the Thermoscript Reverse Transcription System (Invitrogen) according to the manufacturer's instructions. Real-time PCR was performed using Applied Biosystems Power SYBR® Green PCR Master Mix and the Applied Biosystems 7900HT Fast Real-Time PCR System (Applied Biosystems, Carlsbad, CA, USA). Primers were directed against transforming growth factor-β (TGF-β) and platelet-derived growth factor-α and -β subunits (PDGF-α and -β). Primer sequences are listed in Table 1. Gene expression was normalized to 18S.

Detection of Human Cells With Alu Sequences. Total gDNA was isolated from the interphase of the above-mentioned TRIzol preparation according to manufacturer's instructions. The presence of human material in mouse lungs was detected by PCR for *Alu* sequences as previously described (41). Human placental gDNA (5 ng) was used as a positive control, and 10 ng of mouse lung gDNA was used for screening.

In Vitro Studies

To assess direct effects of hAECs on fibroblasts, we performed a series of coculture experiments using primary mouse lung fibroblasts. In these, we analyzed the effects of hAECs on the proliferation, collagen production, and matrix metalloproteinase (MMP) activity of primary lung fibroblasts.

Isolation and Culture of Primary Mouse Lung Fibroblasts. Fibroblasts were isolated from the lungs of C57Bl6 mice as previously described (9). Briefly, lungs were minced into 1-mm pieces and digested for 30 min at 37° with

Table 1. Primer Sequences

Gene of Interest	Sequence
TGF-β	Forward: AGC CTG GAC ACA CAG TAC
	Reverse: TGC ACT TGC AGG AGC GCA C
PDGF-α	Forward: TCA ATT TTG GCT TCT TCC TGA
	Reverse: TAA CAC CAG CAG CGT CAA GT
PDGF-β	Forward: GAA GAT CAT CAA AGG AGC GG
	Reverse: CCT TCC TCT CTG CTG CTA CC
18S	Forward: GTC TGT GAT GCC CTT AGA TGT C
	Reverse: AAG CTT ATG ACC CGC ACT TAC
Alu	Forward: GTC AGG AGA TCG AGA CCA TCC C
	Reverse: TCC TGC CTC AGC CTC CCA AG

TGF, transforming growth factor; PDGF, platelet-derived growth factor.

0.5 mg/ml collagenase A and 10 μg/ml DNase I (both from Roche Applied Sciences, Indianapolis, IN, USA) in serum-free Dulbecco's modified Eagle's medium–high glucose (DMEM-HG; Invitrogen). Cells were separated from the digested tissue by passing the suspension through a 70-μm nylon filter (BD Falcon, San Jose, CA, USA). The single cell suspension was then washed in DMEM-HG containing 10% (v/v) FBS (Invitrogen) and 1% (v/v) penicillin–streptomycin (Invitrogen). The primary lung fibroblasts were then expanded in culture using the same culture medium and used at passage 2 for coculture experiments.

Coculture Studies. Primary mouse lung fibroblasts were cultured in six-well culture-treated polystyrene plates (BD Falcon) at a seeding density of 8,000 cells/cm^2. At the beginning of the study (0 h), hAECs were transferred to 0.4 mm polyethylene terephthelate (PET) cell culture inserts (BD Falcon). Fibroblasts were cultured in triplicate for each endpoint, with exposure to three hAEC donor cell lines. hAECs were seeded at a 3:1 ratio with fibroblasts. Where applicable, fibroblasts were cultured in the presence of 5 ng/ml recombinant human TGF-β (R&D Systems, Minneapolis, MN, USA).

Proliferation of fibroblasts was assessed by MTS assay (Promega Corporation, Madison, WI, USA). Collagen production was measured using a Sircol assay (Biocolor Ltd., Carrickfergus, County Antrim, UK) according to the manufacturer's instructions. Myofibroblast transformation was determined by immunostaining for α-SMA. Using the same coculture conditions as described above, fibroblasts were plated on Thermanox® coverslips (Nunc, Rochester, NY, USA), which were then fixed in ice-cold methanol prior to blocking with serum-free protein block (Dako). Coverslips were then stained with a polyclonal antibody against α-SMA and a universal LSAB$^+$ kit (Dako, Campbellfield, Victoria, Australia). Representative images were taken at 200× magnification with unresized cropped insets. Gene expressions for TGF-β, PDGF-α, and PDGF-β were determined by real-time PCR as described above. RNA was isolated from fibroblasts after 24 h coculture. Primer sequences are listed in Table 1. Gene expression of each marker was normalized to 18S.

Matrix Metalloproteinase Activity Assay. Culture supernatants were collected from each well and concentrated from an original volume of 1 ml to a final volume of 80 μl using the miVac Duo centrifugal concentrator (Genevac, Ipswich, Suffolk, UK). Ten microliters of each concentrated culture supernatant was then loaded onto a 12% gelatin zymogram gel (Invitrogen) and developed according to manufacturer's instructions. Recombinant MMP-2 and MMP-9 (R&D Systems) were used as controls and with the molecular weight markers (Invitrogen) help confirm the expected band sizes. Images were taken using the Chemi Doc XRS$^+$ (Bio-Rad Laboratories).

Statistical Analyses

Results are presented separately for the two in vivo experiments. Data are presented as mean ± SEM. In vivo data were analyzed using two-way single- or repeated-measures ANOVA, as appropriate, with GraphPad Prism (v5.0a for Mac OS X, GraphPad Software, La Jolla, USA). Post hoc comparisons were performed using the Bonferroni test. In vitro data were analyzed with two-way ANOVA or Mann–Whitney *U* test. Statistical significance was accepted for $p<0.05$.

RESULTS

In Vivo Studies

Body Weights and Survival. All mice in all groups survived the experimental protocols. Compared to saline controls, animals exposed to IN bleomycin had significantly reduced body weight from D2 ($p<0.0001$) (Fig. 2). The administration of hAECs, whether at D7 or D14, did not mitigate the bleomycin-related weight loss (Fig. 2A, B). Representative images of H&E and Sirius Red-stained lung sections from each group are shown in Figures 3 and 4, respectively. Compared to saline controls, at day 14 (and 21) bleomycin significantly increased lung tissue density ($p<0.0001$) (Fig. 5A, B), lung area fraction of collagen ($p=0.0008$) (Fig. 5C, D), and α-SMA protein ($p=0.03$) (Fig. 5E, F). The administration of hAECs at D7 had no effect on these bleomycin-induced changes such that, compared to controls, lung tissue density remained increased and not significantly different to bleomycin controls ($p<0.0001$ and $p=0.7$ respectively) (Fig. 5A), lung collagen remained increased and not different to bleomycin controls ($p=0.009$ vs. saline controls, $p=0.5$ vs. bleomycin controls) (Fig. 5C), and α-SMA protein expression remained increased and not different from bleomycin controls ($p=0.04$ vs. controls, $p=0.6$ vs. bleomycin controls) (Fig. 5E).

In contrast, at D21 while bleomycin still significantly increased tissue density, pulmonary collagen and α-SMA compared to saline controls [($p<0.0001$) (Fig. 5B); ($p=0.0001$) (Fig. 5D); ($p=0.03$) (Fig. 5F)], the administration of hAECs at D14 significantly reduced lung tissue density ($p<0.0001$ vs. bleomycin controls) (Fig. 5A), lung collagen content ($p=0.002$ vs. bleomycin controls) (Fig. 5D), and α-SMA protein levels ($p=0.04$ vs. bleomycin controls) (Fig. 5F) at D21. Lung tissue density at D21 following hAEC administration on D14 remained higher than saline controls ($p<0.0001$) (Fig. 5A), while collagen content and α-SMA protein levels were normalized by hAEC administration ($p=0.3$ vs. saline controls) (Fig. 5D) and ($p=0.8$ vs. saline controls) (Fig. 5F).

Lung Inflammation and Fibroblast Activation. Compared to controls, bleomycin significantly increased the lung area fraction of CD45-positive cells at both D14 ($p=0.01$) (Fig. 6A) and D21 ($p=0.02$) (Fig. 6B). The administration of

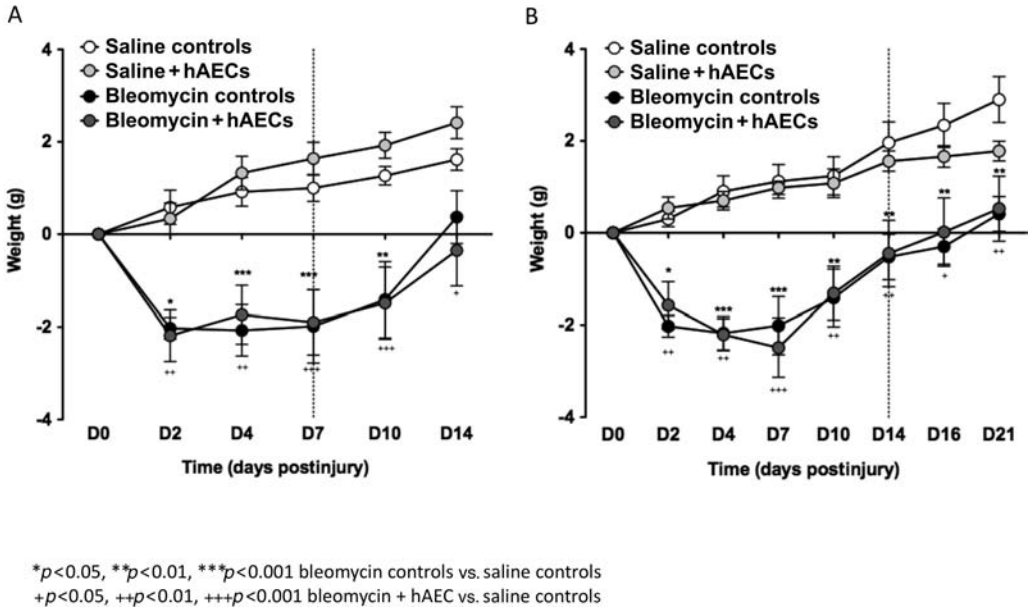

Figure 2. Changes in body weight over time. Administration of bleomycin resulted in a significant reduction in body weight by D2, which remained significantly lower than control by D21. Administration of hAECs at D7 following bleomycin treatment did not normalize body weight. The body weights of bleomycin challenged animals treated with hAEC remained significantly lower compared to that of the saline treated cohort. Administration of hAECs at D14 did not alter weight loss induced by bleomycin by the end of the experiment at D21. *$p<0.05$, **$p<0.01$, ***$p<0.001$ bleomycin + hAEC versus saline controls, +$p<0.05$, ++$p<0.01$, +++$p<0.001$ bleomycin + hAEC versus saline controls. ○, saline controls; ●, saline + hAECs; ●, bleomycin controls; ●, bleomycin + hAECs; dotted lines correspond to hAEC administration.

hAECs at D7 significantly further increased the number of CD45 positive cells at D14 ($p=0.04$ vs. bleomycin controls; $p<0.0001$ vs. saline controls) (Fig. 6A), while the administration of hAECs at D14 significantly reduced the number of CD45-positive cells at D21 compared to bleomycin controls ($p=0.004$) (Fig. 6B) to a level comparable to saline controls ($p=0.9$) (Fig. 6B).

Figure 7 shows the effects of transplantation on TGF-β levels. Compared to saline controls, bleomycin significantly increased the expression of TGF-β ($p=0.005$) (Fig. 7A), PDGF-α ($p=0.0008$) (Fig. 7C), and PDGF-β ($p=0.0003$) (Fig. 7E) mRNA transcription at D14. This effect was prevented by the administration of hAECs at D7 ($p<0.0001$ vs. bleomycin controls, all genes; $p=0.08$, $p=0.3$, $p=0.05$ vs.

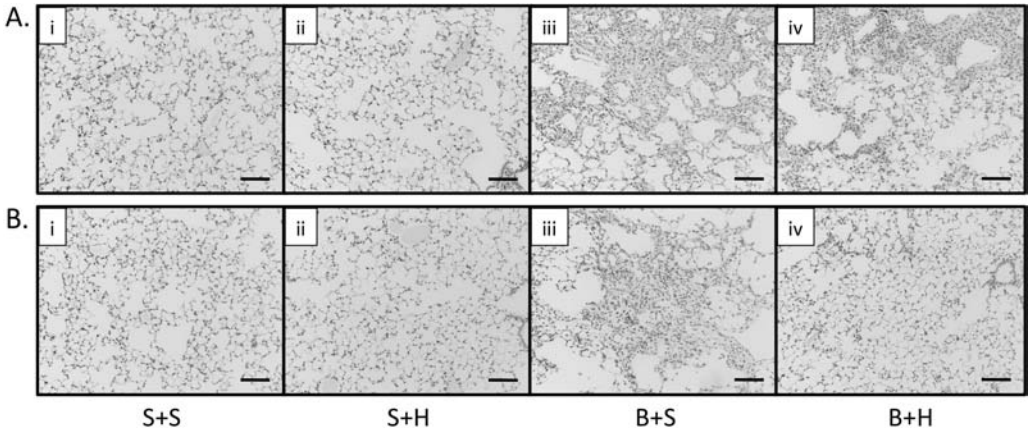

Figure 3. Representative images of lung structure. Lung images (200×) of hematoxylin and eosin (H&E)-stained sections from Experiment 1 – D7 administration cohort (A) and Experiment 2 – D14 administration cohort (B): i. Saline (control; S+S), ii. Saline + hAECs (S+H), iii. Bleomycin alone (B+S), iv. Bleomycin + hAECs (B+H). Scale bars: 100 μm.

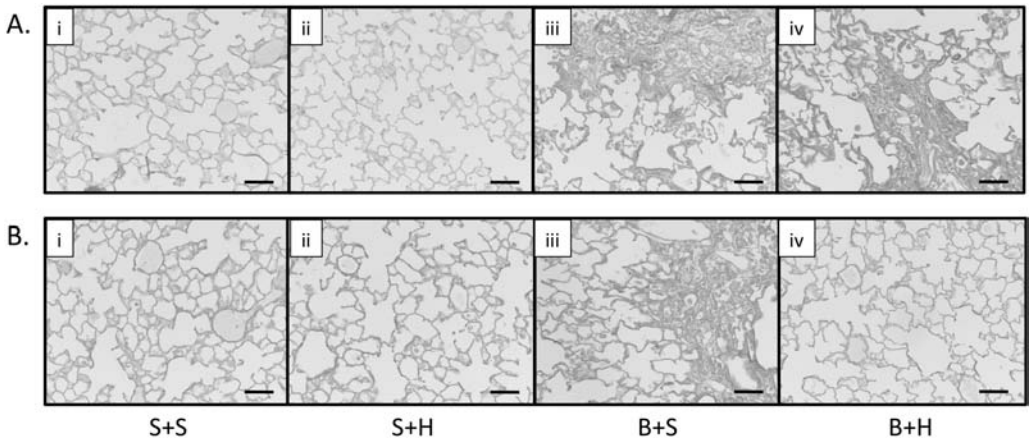

Figure 4. Representative images of collagen staining. Lung images (400×) of Sirius Red-stained sections from D7 administration cohort (A) and D14 administration cohort (B): i. Saline (control), ii. Saline + hAECs, iii. Bleomycin alone, iv. Bleomycin + hAECs. Scale bars: 100 μm.

saline controls, respectively) (Fig. 7A, C, E). At D21, the expression of TGF-β ($p = 0.007$) (Fig. 7B) and PDGF-β ($p = 0.006$) (Fig. 7F) but not PDGF-α mRNA in the lungs of bleomycin control animals remained significantly higher compared to saline controls. The administration of hAECs at D14 normalized TGF-β mRNA expression at D21 ($p < 0.0001$ vs. bleomycin controls; $p = 0.05$ vs. saline controls) (Fig. 7A) but resulted in an intermediate level of PDGF-β mRNA expression that was not statistically different to either bleomycin alone or saline controls ($p = 0.3$ and $p = 0.06$, respectively) (Fig. 7F). No human DNA was found to be present in any of the samples collected when total gDNA from mouse lungs were analyzed for *Alu* sequences (data not shown).

In Vitro Studies

Fibroblast Proliferation, MMP Activity, and Collagen Production. Coculture of primary mouse lung fibroblasts with hAECs significantly reduced fibroblast proliferation, regardless of the presence or absence of TGF-β (Fig. 8A, B). Coculture with hAECs also significantly reduced fibroblast collagen production in the absence ($p < 0.001$) (Fig. 8C) and presence of TGF-β ($p < 0.01$) (Fig. 8D) at 72 h. hAECs did not directly alter the activity of MMP-2 and MMP-9 in primary mouse lung fibroblasts (Fig. 9). Representative images of α-SMA immunostained primary lung fibroblasts are shown in Figure 10. hAEC coculture reduced α-SMA staining in primary mouse fibroblasts by 72 h regardless of the presence of TGF-β.

Fibroblast Gene Expression. To determine whether hAEC coculture directly altered gene expression of growth factors associated with fibroblast proliferation and activation, we performed qPCR on primary mouse fibroblasts with and without hAECs and in the presence or absence of TGF-β. In the absence of exogenous TGF-β, hAEC coculture significantly increased fibroblast expression of profibrotic cytokines TGF-β, PDGF-α, and PDGF-β ($p < 0.0001$, $p < 0.005$, and $p < 0.001$, respectively) (Fig. 11). However, in the presence of exogenous TGF-β, hAEC coculture significantly reduced expression of PDGF-β ($p < 0.05$) but did not affect expression of TGF-β and PDGF-α.

DISCUSSION

In this study, we have explored the ability of hAECs to repair established lung injury and, with a view to understanding mechanisms of action of hAECs, we have examined whether they have any direct effects on lung fibroblasts. We have shown that hAECs are indeed capable of repairing established lung injury and that this is independent of engraftment. hAECs can also directly alter fibroblast proliferation and activity. Specifically, the administration of hAECs to mice with established bleomycin-induced lung damage reduces pulmonary inflammation and key aspects of lung fibrosis including lung tissue density, collagen content, and α-SMA expression. However, critically, this response appears to be dependent on the timing of cell administration relative to the injury. The administration of hAECs was reparative only when delivered during the fibrotic phase of injury at day 14 and not when administered earlier at day 7, during a time of peak inflammation. This suggests that hAEC-mediated lung repair may be dependent on specific host immune mediators within the pulmonary microenvironment that fluctuate throughout the acute-to-chronic inflammatory response. These observations extend the understanding of hAECs as a potential therapy for lung disease, demonstrating that they are not only capable of preventing acute lung injury (33,35,44) but that they can facilitate repair once established.

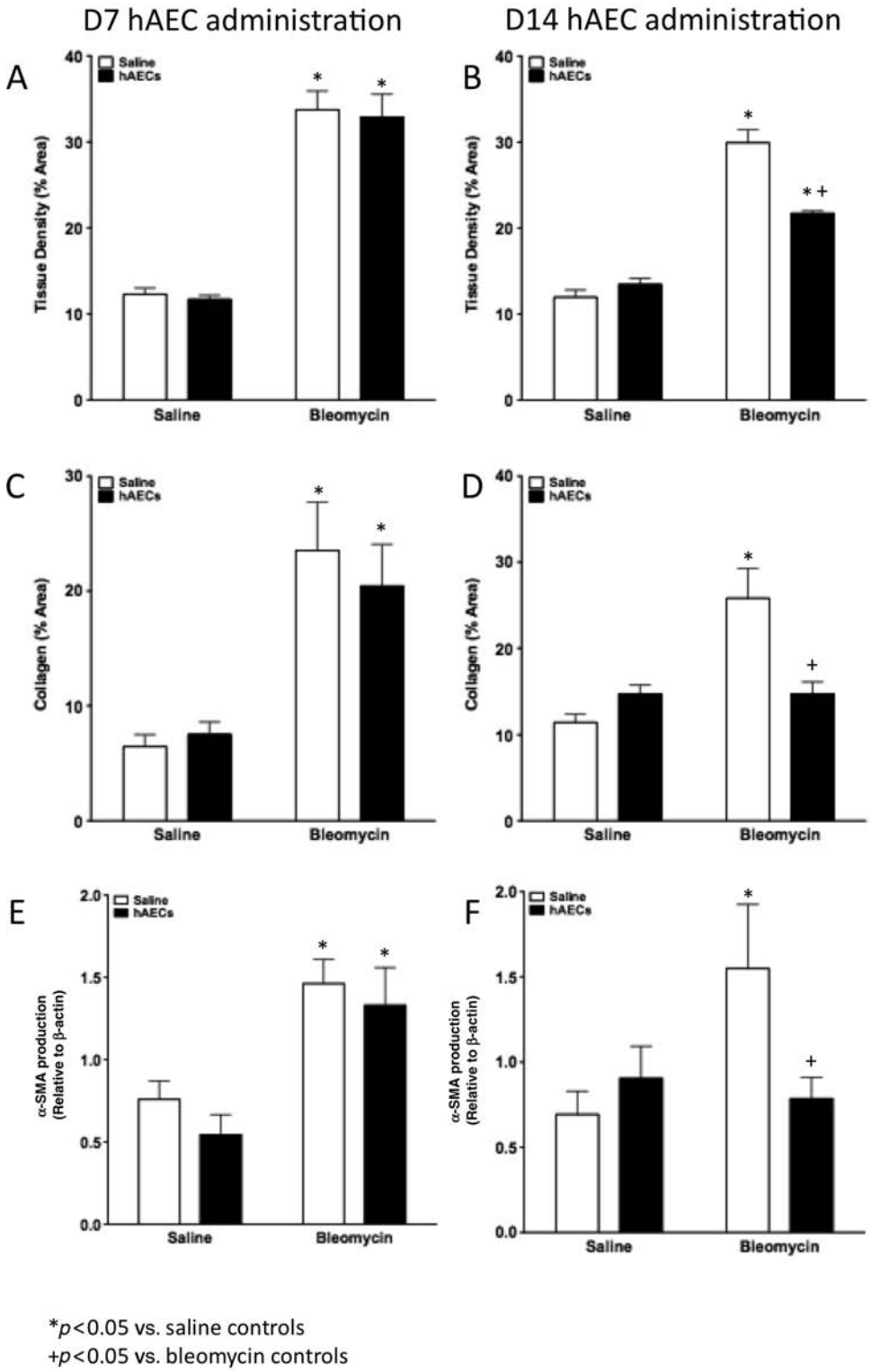

Figure 5. Quantification of structural changes. Bleomycin significantly increased tissue density (A), collagen content (C), and α-smooth muscle actin (α-SMA) expression (E) by D14. Administration of hAECs at D7 did not result in any lung repair. Bleomycin significantly increased tissue density (B), collagen content (D), and α-SMA expression (F) by D21. Administration of hAECs at D14 significantly reduced tissue density and normalized collagen content and α-SMA expression (*$p<0.05$ vs. saline controls; +$p<0.05$ vs. bleomycin controls).

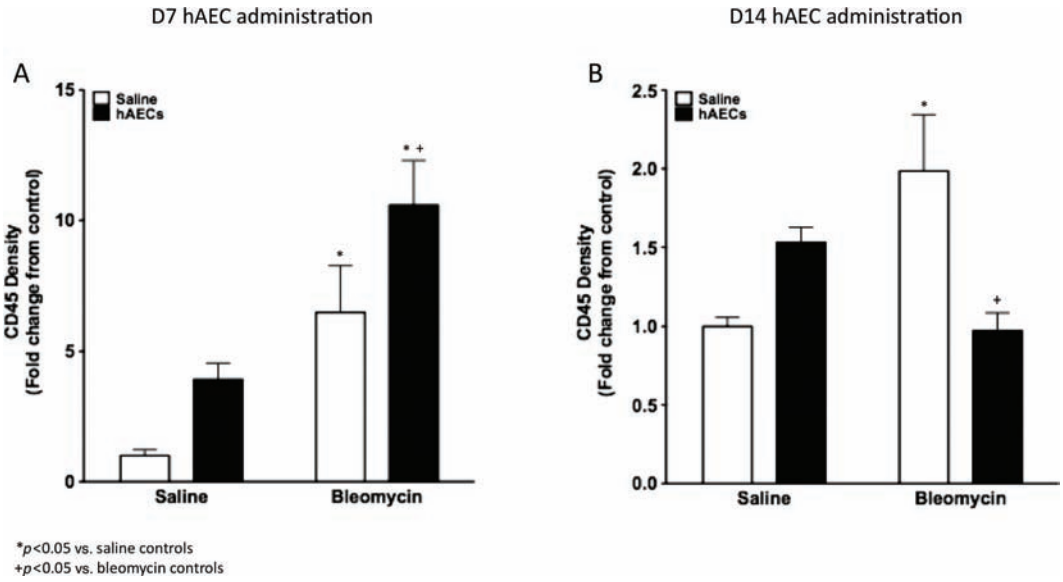

Figure 6. Inflammatory cell infiltrates. Bleomycin significantly increased cluster of differentiation 45 (CD45) staining by D14 (A). Administration of hAECs at D7 further increased CD45 staining compared to control. Bleomycin significantly increased CD45 staining by D21 (B). Administration of hAECs at D14 significantly reduced CD45 staining (*$p<0.05$ vs. saline controls; $^{+}p<0.05$ vs. bleomycin controls).

It is important to understand why hAECs facilitate repair of established lung injury when administered 14 days, but not 7 days, after bleomycin. This may be, at least in part, attributed to the temporal nature of the inflammatory events triggered by bleomycin. The bleomycin mouse model of lung injury has been previously described to involve fluxes in immune cell types entering the lung following the initial challenge including an initial increase in recruitment of macrophages and T lymphocytes into the lung (18,25,35). During this phase, the normal balance between T-helper 1 (Th1) and T-helper 2 (Th2) lymphocytes and between classically (M1) and alternatively activated (M2) macrophages is disturbed resulting in polarization of immune cells to the profibrotic Th2/M2 phenotypes. This is associated with enhanced production of fibroblast-activating cytokines interleukin (IL)-4, IL-10, IL-13, monocyte chemotactic protein-1 (MCP-1), found in inflammatory zone 1 (FIZZ1) and TGF-β (15,25) that in turn are thought to stimulate the differentiation of local fibroblasts and circulating fibrocytes to their activated myofibroblast derivatives. The end effect is parenchymal destruction and generation of pathological fibroblastic foci, leading to scarring (18,31,35). The different outcomes we observed following administration of hAECs at either D7 or D14 following bleomycin are likely to relate to the different immune cell environments within the lung at those time points.

In this regard, it was interesting to note that while the administration of hAECs at D14 after bleomycin was associated with both a reduction in lung leucocytes and in lung injury at D21, the administration of hAECs at D7 increased lung leucocyte number and was not associated with lung repair. This suggests that the reparative effects of hAECs may depend upon modifying the host inflammatory response. This supports other recent reports that immune modulation is the likely mechanism by which hAECs exert their reparative effects (35,44). We have previously shown that hAECs attenuate the acute immune response to bleomycin preventing pulmonary fibrosis if delivered within the first 24 h (35). Prevention of injury was associated with fewer neutrophils and macrophages in the lung and reduced gene expression of early inflammatory cytokines tumor necrosis factor-α (TNF-α), IL-1, IL-6, and interferon-γ (IFN-γ) (33,35). We also noted a similar effect in fetal sheep where alveolar simplification and abnormal lung compliance due to intra-amniotic lipopolysaccharide (LPS) exposure was prevented by hAEC administration (44). These effects were accompanied by a reduction in proinflammatory cytokines, as well as an enhanced gene expression of surfactant proteins A and C, which have anti-inflammatory capabilities. Together, the previous and current studies confirm that hAECs can protect against and repair lung injury by mitigating pulmonary inflammation.

If this is the case, then our observation that D7 administration of hAECs increased lung leukocyte number may be of concern. Polymorphic responses to hAECs, human amniotic mesenchymal stem cells (hAMSCs), and bone marrow stem cells (BMSCs) have previously been reported in coculture experiments with peripheral blood mononuclear cells (PBMCs), despite the low immunogenicity of each cell type (28,39,46). Further, in a fetal

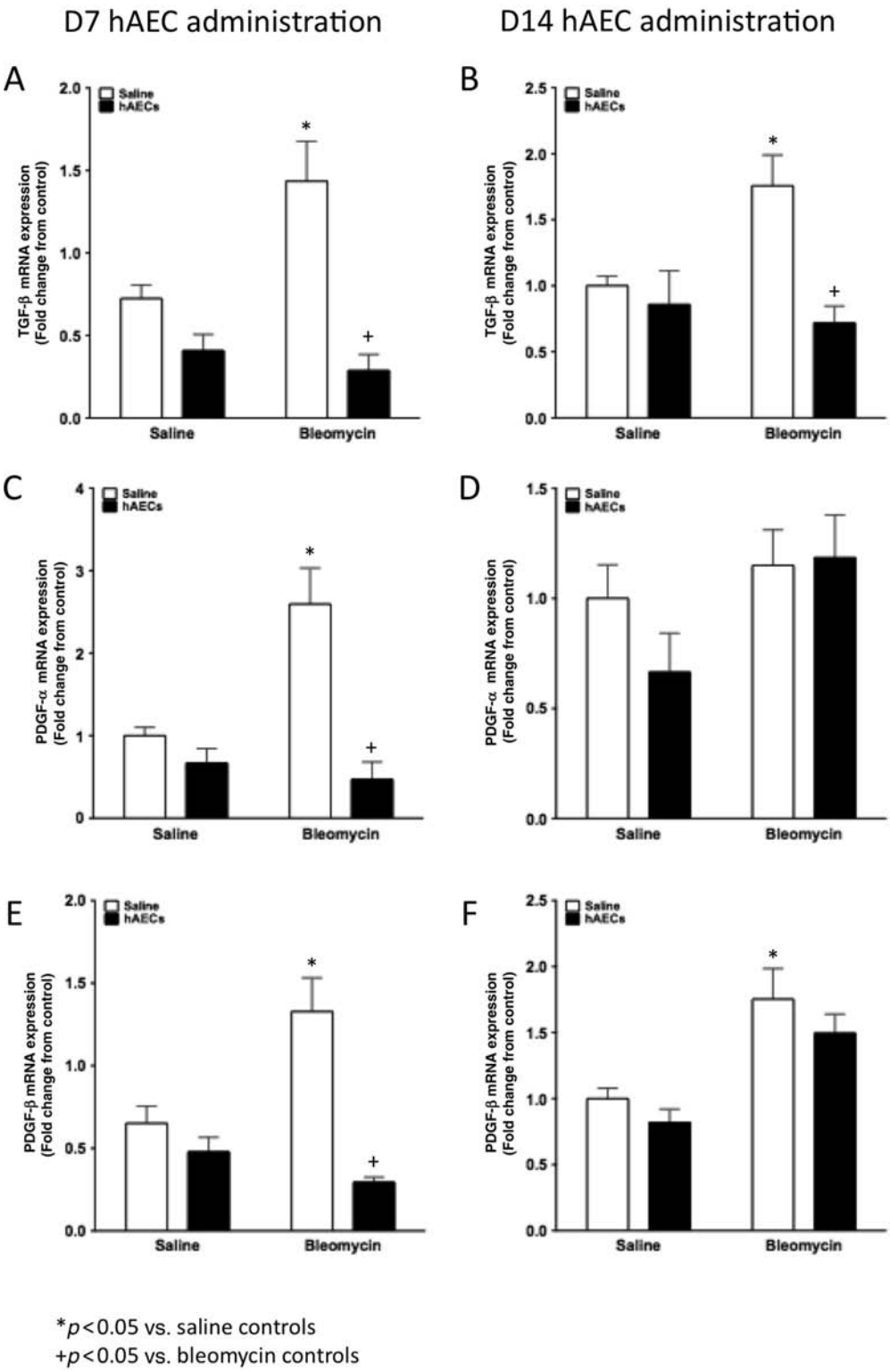

Figure 7. Inflammatory cytokine gene expression. Bleomycin significantly increased transforming growth factor (TGF)-β (A), platelet-derived growth factor (PDGF)-α (C), and PDGF-β (E) gene expression by D14. Administration of hAECs at D7 significantly reduced expression of all cytokines. Bleomycin significantly increased TGF-β (B) and PDGF-β (F) gene expression by D21. Administration of hAECs at D14 significantly reduced TGF-β expression by D21 but did not alter gene expression of PDGF-β. There were no differences in PDGF-α (D) gene expression between any groups at D21 (*$p<0.05$ vs. saline controls; +$p<0.05$ vs. bleomycin controls).

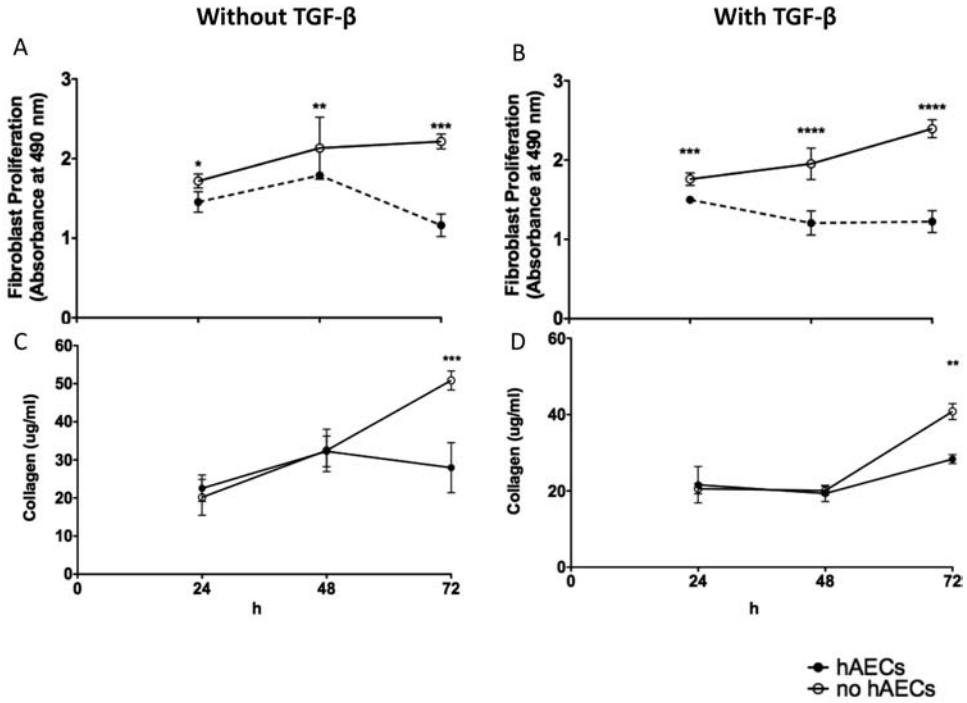

Figure 8. Fibroblast proliferation and collagen synthesis following hAEC coculture. Coculture with hAECs significantly reduced proliferation of primary mouse lung fibroblasts regardless of the absence (A) or presence (B) of recombinant TGF-β (*$p<0.05$, **$p<0.01$, ***$p<0.001$, ****$p<0.0001$). ●, with hAECs; ○, without hAECs. hAECs also significantly reduced collagen synthesis by fibroblasts following 72 h of coculture regardless of the absence (C) or presence (D) of recombinant TGF-β (**$p<0.01$, ***$p<0.001$).

sheep model of lung injury we have shown that hAECs can increase lung leukocytes (44). However, in that study, the leukocytosis was associated with a reduction in proinflammatory cytokines TNF-α, IL-1, and IL-6 (44), and in the present study, TGF-β, PDGF-α, and PDGF-β levels were reduced despite increased white cell numbers. This is important because these proinflammatory and profibrotic cytokines are thought to underlie the injury. Thus, it is possible that, while hAECs recruit inflammatory cells to the lung, at least during the acute phase of injury, they appear able to modulate the cells and reduce inflammatory signaling. Indeed, it is possible that hAEC-mediated repair involves recruitment of specific subsets of inflammatory cells, such as macrophages and T lymphocytes, dependent on the immune environment into which they have been introduced (15). In this regard, hAECs express HLA-G, an anti-inflammatory antigen known to suppress $CD4^+$ T-cell proliferation and support apoptosis of $CD8^+$ T-cells (27). These characteristics may represent a capacity of hAECs to modulate T-cell responses and reestablish the Th1/Th2 balance to enable coordinated lung repair. It would certainly be worthwhile examining the ability of hAECs to modulate Th1/Th2 balance as has been previously shown with MSCs (48,49).

That the D7 administration of hAECs reduced expression of TGF-β, PDGF-α, and PDGF-β by D14 but did not result in augmented lung repair suggests that this effect is either not critical for repair or, on its own, is insufficient for repair. Further studies will be required to tease out the relative roles of the cytokine signaling and the inflammatory cells. However, it was interesting that, in the current study, we observed that hAECs directly increased gene transcription of these profibrotic cytokines in lung fibroblasts in the absence of exogenous TGF-β but had little effect on them in the presence of TGF-β. While increased gene expression of profibrotic cytokines is in line with recent reports where amniotic MSCs have been observed to express TGF-β (19), the apparent lack of effect in the presence of TGF-β suggests that hAECs may act on other cell types rather than fibroblasts. This includes inflammatory cells such as macrophages, which have been shown to be critical in the development of bleomycin induced lung fibrosis, where TGF-β and PDGF produced by macrophages regulate collagen production by lung fibroblasts (20). However, unlike previous reports on cord blood and bone marrow-derived MSC induction on fibroblast activation (40), hAECs had a suppressive effect on fibroblast activation, proliferation and collagen production. Our findings are in line with previous reports of amnion stromal cells and extract, which have consistently been shown to reduce myofibroblast differentiation and α-SMA production in cultured fibroblasts (21,24,42,43).

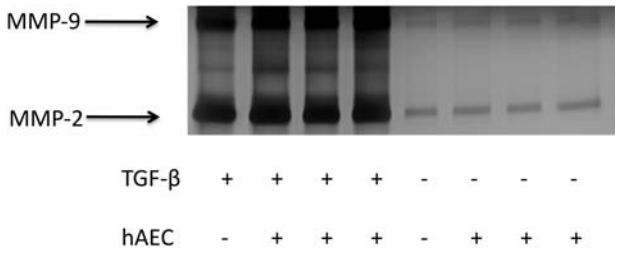

Figure 9. MMP activity in primary mouse lung fibroblasts following hAEC coculture. Representative image of gelatin zymography. Coculture with hAECs did not alter the activity of matrix metalloproteinase-2 (MMP-2) and MMP-9 produced by primary lung fibroblasts in vitro regardless of the presence of TGF-β.

We were a little surprised that hAECs did not appear to alter the activity of either MMP-2 and -9 in primary mouse lung fibroblasts, particularly as we have previously shown that hAEC administration in vivo increased activation of MMP-2 and reduced production of tissue inhibitors of matrix metalloproteinase (TIMPs) (33). MMPs are extracellular enzymes that play a degradative role for the breakdown of collagen and resolution of scarring. However, MMPs in the lung are secreted by many cell types including macrophages (22), neutrophils (12), bronchial epithelia (47), and fibroblasts (10). Therefore, it is possible that hAECs alter MMP activity in other cell types, thus contributing to an overall increase in MMP activity as previously reported (33) resulting in reduced lung fibrosis. It would also be important to determine in future studies whether hAECs had any effects on the activity of TIMPs in the various cell types. This is particularly relevant since TIMP activity has been previously reported to be downregulated and in tandem, MMP-2 activity upregulated, in whole lung lysates of bleomycin challenged mice following administration of hAECs and MSCs from Wharton's Jelly (32,33). Together, our data suggest that the antifibrotic effects of hAECs may be attributed to direct effects on fibroblasts by altering their proliferation rate, activation state, and collagen production but independent of the production of active MMP-2 and -9 by fibroblasts. These effects were also independent of TGF-β and PDGF gene transcription, although the significance of their respective signaling pathways merits further investigation.

Last, that all of the in vivo effects reported in the current study were exerted by hAECs without engraftment supports our previous findings in acute injury (34,35) and suggests that the likely mechanisms of action are via circulating mediators, not requiring direct cell-to-cell contact. This notion is further supported by previous studies demonstrating that conditioned media from amnion cells are able to prevent progression of bleomycin-induced lung fibrosis (5) and promote the rate of wound closure and break strength (13). If this is the case, then defining what humoral factors are involved may lead to the development

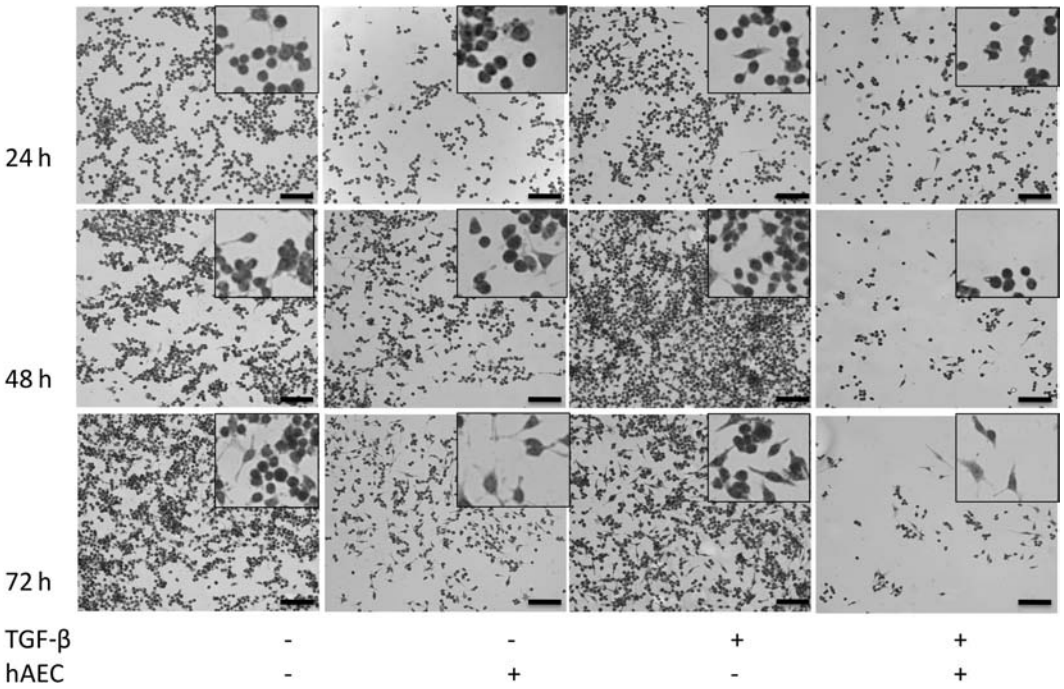

Figure 10. α-SMA expression by primary mouse lung fibroblast. Representative images of α-SMA immunohistochemical staining of primary mouse lung fibroblasts following 24, 48, and 72 h coculture with hAECs. Images were taken at 200× magnification. Scale bar: 100 μm. Inset images are cropped and resized versions of the same image.

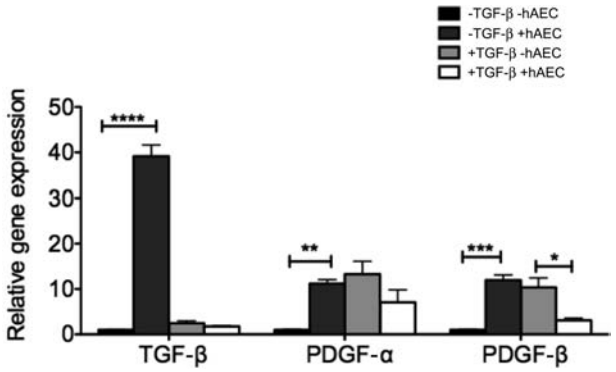

Figure 11. Gene expression of profibrotic cytokines by primary mouse lung fibroblasts. Coculture with hAECs significantly increased fibroblast expression of TGF-β, PDGF-α, and PDGF-β in the absence of recombinant TGF-β. In the presence of TGF-β, fibroblasts significantly reduced gene expression of PDGF-β. $^{**}p<0.05$, $^{**}p<0.01$, $^{***}p<0.001$, $^{****}p<0.0001$.

of novel pharmacological therapies rather than cell-based therapies.

In conclusion, this study is the first to demonstrate a capacity of hAECs to repair established lung fibrosis in an immune-competent animal and to demonstrate a time-dependent response of hAECs in achieving lung repair. Our study ushers the way for future studies to explore potential pathways, such as those of macrophage and T-cell responses, which by this account appear to be more important in pulmonary fibrosis than the influence of fibroblasts.

ACKNOWLEDGMENTS: This research was funded by a grant from the National Health and Medical Research Council of Australia (NHMRC) and supported by the Victorian Government's Operational Infrastructure Support Program. The authors declare no conflict of interest.

REFERENCES

1. Akle, C. A.; Adinolfi, M.; Welsh, K. I.; Leibowitz, S.; McColl, I. Immunogenicity of human amniotic epithelial cells after transplantation into volunteers. Lancet 2(8254):1003–1005; 1981.
2. Bose, B. Burn wound dressing with human amniotic membrane. Ann. R. Coll. Surg. Engl. 61(6):444–447; 1979.
3. Bourke, S. J. Interstitial lung disease: Progress and problems. Postgrad. Med. J. 82(970):494–499; 2006.
4. Cargnoni, A.; Gibelli, L.; Tosini, A.; Signoroni, P. B.; Nassuato, C.; Arienti, D.; Lombardi, G.; Albertini, A.; Wengler, G. S.; Parolini, O. Transplantation of allogeneic and xenogeneic placenta-derived cells reduces bleomycin-induced lung fibrosis. Cell Transplant. 18(4):405–422; 2009.
5. Cargnoni, A.; Ressel, L.; Rossi, D.; Poli, A.; Arienti, D.; Lombardi, G.; Parolini, O. Conditioned medium from amniotic mesenchymal tissue cells reduces progression of bleomycin-induced lung fibrosis. Cytotherapy 14(2):153–161; 2011.
6. Cerny, L.; Torday, J. S.; Rehan, V. K. Prevention and treatment of bronchopulmonary dysplasia: Contemporary status and future outlook. Lung 186(2):75–89; 2008.
7. Diaz-Prado, S.; Muinos-Lopez, E.; Hermida-Gomez, T.; Rendal-Vazquez, M. E.; Fuentes-Boquete, I.; de Toro, F. J.; Blanco, F. J. Multilineage differentiation potential of cells isolated from the human amniotic membrane. J. Cell. Biochem. 111(4):846–857; 2010.
8. Dua, H. S.; Gomes, J. A.; King, A. J.; Maharajan, V. S. The amniotic membrane in ophthalmology. Surv. Ophthalmol. 49(1):51–77; 2004.
9. Dunsmore, S. E.; Martinez-Williams, C.; Goodman, R. A.; Rannels, D. E. Composition of extracellular matrix of type 2 pulmonary epithelial cells in primary culture. Am. J. Physiol. 269(6 Pt 1):L754–765; 1995.
10. Eickelberg, O.; Kohler, E.; Reichenberger, F.; Bertschin, S.; Woodtli, T.; Erne, P.; Perruchoud, A. P.; Roth, M. Extracellular matrix deposition by primary human lung fibroblasts in response to TGF-β1 and TGF-β3. Am. J. Physiol. 276(5 Pt 1):L814–L824; 1999.
11. Fahey, M. C.; Wallace, E. M. Stem cells: Research tools and clinical treatments. J. Paediatr. Child Health 47(9): 672–675; 2011.
12. Ferry, G.; Lonchampt, M.; Pennel, L.; de Nanteuil, G.; Canet, E.; Tucker, G. C. Activation of MMP-9 by neutrophil elastase in an in vivo model of acute lung injury. FEBS Lett. 402(2–3):111–115; 1997.
13. Franz, M. G.; Payne, W. G.; Xing, L.; Naidu, D. K.; Salas, R. E.; Marshall, V. S.; Trumpower, C. J.; Smith, C. A.; Steed, D. L.; Robson, M. C. The use of amnion-derived cellular cytokine solution to improve healing in acute and chronic wound models. Eplasty 8:e21; 2008.
14. Ganatra, M. A. Amniotic membrane in surgery. J. Pak. Med. Assoc. 53(1):29–32; 2003.
15. Homer, R. J.; Elias, J. A.; Lee, C. G.; Herzog, E. Modern concepts on the role of inflammation in pulmonary fibrosis. Arch. Pathol. Lab. Med. 135(6):780–788; 2011.
16. Hori, J.; Wang, M.; Kamiya, K.; Takahashi, H.; Sakuragawa, N. Immunological characteristics of amniotic epithelium. Cornea 25(10 Suppl 1):S53–58; 2006.
17. Ilancheran, S.; Michalska, A.; Peh, G.; Wallace, E. M.; Pera, M.; Manuelpillai, U. Stem cells derived from human fetal membranes display multilineage differentiation potential. Biol. Reprod. 77(3):577–588; 2007.
18. Izbicki, G.; Segel, M. J.; Christensen, T. G.; Conner, M. W.; Breuer, R. Time course of bleomycin-induced lung fibrosis. Int. J. Exp. Pathol. 83(3):111–119; 2002.
19. Kang, J. W.; Koo, H. C.; Hwang, S. Y.; Kang, S. K.; Ra, J. C.; Lee, M. H.; Park, Y. H. Immunomodulatory effects of human amniotic membrane-derived mesenchymal stem cells. J. Vet. Sci. 13(1):23–31; 2012.
20. Koslowski, R.; Seidel, D.; Kuhlisch, E.; Knoch, K. P. Evidence for the involvement of TGF-β and PDGF in the regulation of prolyl 4-hydroxylase and lysyloxidase in cultured rat lung fibroblasts. Exp. Toxicol. Pathol. 55(4): 257–264; 2003.
21. Lee, S. B.; Li, D. Q.; Tan, D. T.; Meller, D. C.; Tseng, S. C. Suppression of TGF-β signaling in both normal conjunctival fibroblasts and pterygial body fibroblasts by amniotic membrane. Curr. Eye Res. 20(4):325–334; 2000.
22. Lemjabbar, H.; Gosset, P.; Lechapt-Zalcman, E.; Franco-Montoya, M. L.; Wallaert, B.; Harf, A.; Lafuma, C. Over-expression of alveolar macrophage gelatinase B (MMP-9) in patients with idiopathic pulmonary fibrosis: Effects of

steroid and immunosuppressive treatment. Am. J. Respir. Cell Mol. Biol. 20(5):903–913; 1999.
23. Li, H.; Niederkorn, J. Y.; Neelam, S.; Mayhew, E.; Word, R. A.; McCulley, J. P.; Alizadeh, H. Immunosuppressive factors secreted by human amniotic epithelial cells. Invest. Ophthalmol. Vis. Sci. 46(3):900–907; 2005.
24. Li, W.; He, H.; Chen, Y. T.; Hayashida, Y.; Tseng, S. C. Reversal of myofibroblasts by amniotic membrane stromal extract. J. Cell. Physiol. 215(3):657–664; 2008.
25. Lossos, I. S.; Breuer, R.; Shriki, M.; Or, R. Peribronchial lymphocyte activation in bleomycin-induced lung injury. Life Sci. 63(13):1183–1193; 1998.
26. Manali, E. D.; Moschos, C.; Triantafillidou, C.; Kotanidou, A.; Psallidas, I.; Karabela, S. P.; Roussos, C.; Papiris, S.; Armaganidis, A.; Stathopoulos, G. T.; Maniatis, N. A. Static and dynamic mechanics of the murine lung after intratracheal bleomycin. BMC Pulm. Med. 11:33; 2011.
27. McDonald, C.; Siatskas, C.; Bernard, C. The emergence of amnion epithelial stem cells for the treatment of multiple sclerosis. Inflammation and Regeneration 31(3):257–269; 2011.
28. McIntosh, K.; Zvonic, S.; Garrett, S.; Mitchell, J. B.; Floyd, Z. E.; Hammill, L.; Kloster, A.; Di Halvorsen, Y.; Ting, J. P.; Storms, R. W.; Goh, B.; Kilroy, G.; Wu, X.; Gimble, J. M. The immunogenicity of human adipose-derived cells: Temporal changes in vitro. Stem Cells 24(5):1246–1253; 2006.
29. Miki, T.; Lehmann, T.; Cai, H.; Stolz, D. B.; Strom, S. C. Stem cell characteristics of amniotic epithelial cells. Stem Cells 23(10):1549–1559; 2005.
30. Miravitlles, M.; Anzueto, A. Insights into interventions in managing COPD patients: Lessons from the TORCH and UPLIFT studies. Int. J. Chron. Obstruct. Pulmon. Dis. 4: 185–201; 2009.
31. Moeller, A.; Ask, K.; Warburton, D.; Gauldie, J.; Kolb, M. The bleomycin animal model: A useful tool to investigate treatment options for idiopathic pulmonary fibrosis? Int. J. Biochem. Cell Biol. 40(3):362–382; 2008.
32. Moodley, Y.; Atienza, D.; Manuelpillai, U.; Samuel, C. S.; Tchongue, J.; Ilancheran, S.; Boyd, R.; Trounson, A. Human umbilical cord mesenchymal stem cells reduce fibrosis of bleomycin-induced lung injury. Am. J. Pathol. 175(1):303–313; 2009.
33. Moodley, Y.; Ilancheran, S.; Samuel, C.; Vaghjiani, V.; Atienza, D.; Williams, E. D.; Jenkin, G.; Wallace, E.; Trounson, A.; Manuelpillai, U. Human amnion epithelial cell transplantation abrogates lung fibrosis and augments repair. Am. J. Respir. Crit. Care Med. 182(5):643–651; 2010.
34. Murphy, S. V.; Shiyun, S. C.; Tan, J. L.; Chan, S.; Jenkin, G.; Wallace, E. M.; Lim, R. Human amnion epithelial cells do not abrogate pulmonary fibrosis in mice with impaired macrophage function. Cell Transplant. 21(7):1477–1492; 2012.
35. Murphy, S.; Lim, R.; Dickinson, H.; Acharya, R.; Rosli, S.; Jenkin, G.; Wallace, E. Human amnion epithelial cells prevent bleomycin-induced lung injury and preserve lung function. Cell Transplant. 20(6):909–923; 2010.
36. Murphy, S.; Rosli, S.; Acharya, R.; Mathias, L.; Lim, R.; Wallace, E.; Jenkin, G. Amnion epithelial cell isolation and characterization for clinical use. Curr. Protoc. Stem Cell Biol. 13:1E.6.1–1E.6.25; 2010.
37. National Health and Medical Research Council of Australia. Australian code of practice for the care and use of animals for scientific purposes. Canberra, Australia: NH&MRC; 2004.
38. Parolini, O.; Alviano, F.; Bagnara, G. P.; Bilic, G.; Buhring, H. J.; Evangelista, M.; Hennerbichler, S.; Liu, B.; Magatti, M.; Mao, N.; Miki, T.; Marongiu, F.; Nakajima, H.; Nikaido, T.; Portmann-Lanz, C. B.; Sankar, V.; Soncini, M.; Stadler, G.; Surbek, D.; Takahashi, T. A.; Redl, H.; Sakuragawa, N.; Wolbank, S.; Zeisberger, S.; Zisch, A.; Strom, S. C. Concise review: Isolation and characterization of cells from human term placenta: Outcome of the first international Workshop on Placenta Derived Stem Cells. Stem Cells 26(2):300–311; 2008.
39. Potian, J. A.; Aviv, H.; Ponzio, N. M.; Harrison, J. S.; Rameshwar, P. Veto-like activity of mesenchymal stem cells: Functional discrimination between cellular responses to alloantigens and recall antigens. J. Immunol. 171(7):3426–3434; 2003.
40. Salazar, K. D.; Lankford, S. M.; Brody, A. R. Mesenchymal stem cells produce Wnt isoforms and TGF-β1 that mediate proliferation and procollagen expression by lung fibroblasts. Am. J. Physiol. Lung Cell. Mol. Physiol. 297(5):L1002–L1011; 2009.
41. Schneider, T.; Osl, F.; Friess, T.; Stockinger, H.; Scheuer, W. V. Quantification of human Alu sequences by real-time PCR—an improved method to measure therapeutic efficacy of anti-metastatic drugs in human xenotransplants. Clin. Exp. Metastasis 19(7):571–582; 2002.
42. Solomon, A.; Wajngarten, M.; Alviano, F.; Anteby, I.; Elchalal, U.; Pe'er, J.; Levi-Schaffer, F. Suppression of inflammatory and fibrotic responses in allergic inflammation by the amniotic membrane stromal matrix. Clin. Exp. Allergy 35(7):941–948; 2005.
43. Tseng, S. C.; Li, D. Q.; Ma, X. Suppression of transforming growth factor-β isoforms, TGF-β receptor type 2, and myofibroblast differentiation in cultured human corneal and limbal fibroblasts by amniotic membrane matrix. J. Cell. Physiol. 179(3):325–335; 1999.
44. Vosdoganes, P.; Hodges, R. J.; Lim, R.; Westover, A. J.; Acharya, R. Y.; Wallace, E. M.; Moss, T. J. Human amnion epithelial cells as a treatment for inflammation-induced fetal lung injury in sheep. Am. J. Obstet. Gynecol. 205(156): 26–33; 2011.
45. World Health Organisation. World Health Statistics Geneva. http://www.who.int/whosis/whostat/2008/en/index.html. Accessed 20th June 2012.
46. Wolbank, S.; Peterbauer, A.; Fahrner, M.; Hennerbichler, S.; van Griensven, M.; Stadler, G.; Redl, H.; Gabriel, C. Dose-dependent immunomodulatory effect of human stem cells from amniotic membrane: A comparison with human mesenchymal stem cells from adipose tissue. Tissue Eng. 13(6):1173–1183; 2007.
47. Yao, P. M.; Delclaux, C.; d'Ortho, M. P.; Maitre, B.; Harf, A.; Lafuma, C. Cell-matrix interactions modulate 92-kD gelatinase expression by human bronchial epithelial cells. Am. J. Respir. Cell Mol. Biol. 18(6):813–822; 1998.
48. Zhang, X.; Ren, X.; Li, G.; Jiao, C.; Zhang, L.; Zhao, S.; Wang, J.; Han, Z. C.; Li, X. Mesenchymal stem cells ameliorate experimental autoimmune uveoretinitis by comprehensive modulation of systemic autoimmunity. Invest. Ophthalmol. Vis. Sci. 52(6):3143–3152; 2011.
49. Zhou, H. P.; Yi, D. H.; Yu, S. Q.; Sun, G. C.; Cui, Q.; Zhu, H. L.; Liu, J. C.; Zhang, J. Z.; Wu, T. J. Administration of donor-derived mesenchymal stem cells can prolong the survival of rat cardiac allograft. Transplant. Proc. 38(9): 3046–3051; 2006.